J|A|C|S
COMMUNICATIONS

Reconstruction of Cu(100) Electrode Surfaces during Hydrogen Evolution

Hisayoshi Matsushima, Andriy Taranovskyy, Christian Haak, Yvonne Gründer, and
Olaf M. Magnussen*

Institut für Experimentelle und Angewandte Physik, Christian-Albrechts-Universität zu Kiel, 24098 Kiel, Germany

Received May 18, 2009; E-mail: magnussen@physik.uni-kiel.de

The interaction of hydrogen with metal electrode surfaces is of key importance to the hydrogen evolution reaction (HER), one of the most extensively studied electrochemical processes, as well as of considerable relevance to corrosion and electroplating, where it may result in incorporation of hydrogen into the metal. Nevertheless, the structure of electrode surfaces under the conditions of electrochemical hydrogen evolution is largely unknown. Based on studies of H adsorption under ultrahigh vacuum (UHV) conditions,[1,2] the presence of subsurface H in interstitials between the first and second atomic layer of the metal electrode was suggested as a distinct intermediate species in various hydrogen absorption mechanisms.[3,4] However, direct evidence for such subsurface hydrogen in an electrochemical environment is lacking so far.

On single crystal surfaces of transition metals, such as Ni or Cu, hydrogen adsorption from the gas phase has been extensively investigated by UHV surface science and theoretical methods. Specifically, hydrogen was found to often induce a reconstruction of the surface layer under these conditions.[5] In electrochemical environment surface reconstruction likewise is an important, well-studied phenomenon but has up to now only been reported in the absence of chemisorbed species[6] or due to interaction with anions, such as sulfate or halides.[7,8] We here present high-resolution *in situ* scanning tunneling microscopy (STM) results on the Cu(100) surface structure in the hydrogen evolution regime and supplementary electrochemical data, which unambiguously demonstrate that hydrogen-induced reconstructions can also occur at electrochemical interfaces and have a pronounced influence on the electrode reactivity, specifically the HER.

For the studies an *in situ* STM with high temporal resolution was employed. Atomic resolution studies in 0.1 M $HClO_4$ solution reveal only the square lattice of the Cu(100) surface atoms with a lattice distance of $d_{\mathrm{Cu}} = 2.55$ Å in the entire double layer potential range (Figure 1a). Upon decreasing the potential into the hydrogen evolution regime, the sudden formation of characteristic stripe-like structures is observed within less than 0.1 s (Figure 1b). These stripes are oriented in the [011] direction, i.e., parallel to the Cu lattice, and exhibit a minimum distance of $4 \cdot d_{\mathrm{Cu}}$ with respect to each other, whereas along the stripes the Cu lattice spacing is maintained. Larger domains of the new phase with a well-defined minimum stripe separation of $4 \cdot d_{\mathrm{Cu}}$ (Figure 1c,d) are formed by subsequent lateral motion of these structures as well as by nucleation and growth of additional stripes. At sufficiently negative potentials (see below) this surface phase transition occurs within a few seconds (an STM video is available), with local growth rates of individual stripes exceeding 100 nm/s even at the onset of the phase transition.

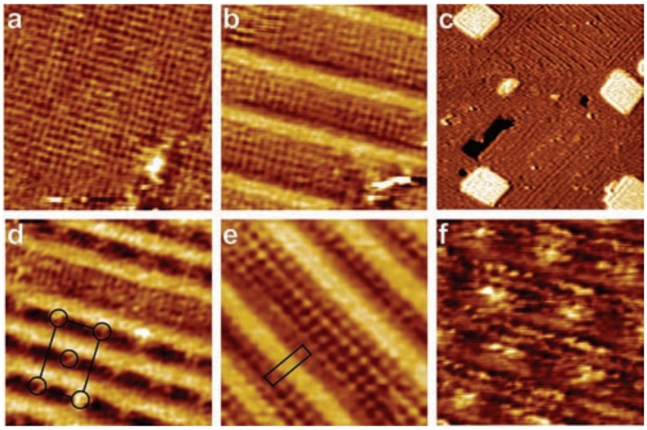

Figure 1. *In situ* STM images of Cu(100) in 0.1 M $HClO_4$ solution. (a,b) Images of a video sequence (6 × 6 nm^2), showing (a) the (1 × 1) lattice at -0.53 V_{SCE} and (b) the same surface area 0.2 s later at -0.64 V_{SCE}. (c−f) Images of (c) the Cu surface morphology (-0.70 V_{SCE}, 16 × 16 nm^2), (d) extended reconstruction domains (-0.68 V_{SCE}, 7.2 × 7.2 nm^2), and (e,f) the reconstruction at high resolution (-0.65 V_{SCE}, 3.5 × 3.5 nm^2 and -0.70 V_{SCE}, 4 × 4 nm^2).

High-resolution images (Figure 1e) reveal that the stripes consist of two parallel elevated rows of surface atoms. The apparent stripe height in constant current STM images is 0.35 Å relative to the neighboring (1 × 1) Cu lattice, suggesting that the atoms in the stripes are displaced from the hollow sites of the underlying substrate lattice. Within larger domains of the new phase two elevated atomic rows alternate with two lower lying rows; i.e., the surface lattice exhibits four rows of atoms per unit cell. Due to the very fast transition and the high image acquisition rates of our STM the thermal drift is negligible, allowing direct comparison of the atomic lattice within this phase to the unreconstructed (1 × 1) lattice at more positive potentials. A detailed analysis reveals a nonuniform spacing of the atomic rows in the superstructure unit cell (indicated by rectangle in Figure 1e). In particular, the two elevated rows exhibit a reduced spacing of only 2.0 ± 0.2 Å, whereas the spacing between the other atomic rows is slightly expanded. These observations can be explained by a local quasi-hexagonal distortion of the Cu surface layer within the elevated rows as illustrated in the model in Figure 2a.

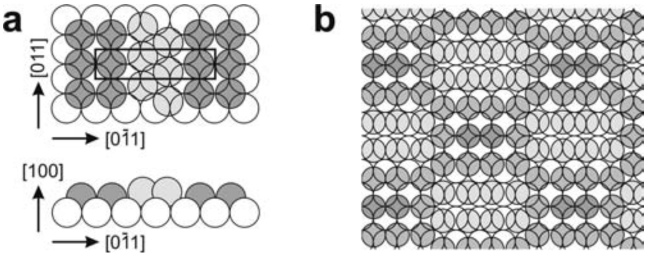

Figure 2. Structural models of the hydrogen-induced surface reconstruction. (a) Local atomic arrangement in isolated reconstruction stripes; (b) schematic model of the Moiré superstructure.

10.1021/ja904033t CCC: $40.75 © 2009 American Chemical Society

In larger domains an additional long-range modulation along the stripe direction with a period of $\sim 6 \cdot d_{Cu}$ is visible (modulation maxima indicated by circles in Figure 1d). This structure can be assigned to a Moiré pattern, caused by an $\sim$20% expansion of the surface lattice in the direction parallel to the stripes, also supported by high-resolution STM images of this phase (Figure 1f). Clear evidence of such a reconstruction of the Cu surface is the characteristic morphological changes during the structural phase transition, similar to those found in other potential-induced surface reconstructions.[6−8] Specifically, the formation of the reconstruction is accompanied by the emergence of roughly square Cu monolayer islands on the initial smooth Cu(100) terraces (Figure 1c, light areas), formed by Cu adatoms expelled onto the surface during the phase transition. Vice versa, monoatomically deep holes (dark areas in Figure 1c) are observed after the reverse transition to the (1×1) phase due to the concomitant lattice contraction. The Moiré pattern can be rationalized by a $c(p \times 8)$ superstructure with $p \approx 1.2$ as shown schematically in Figure 2b. In this structure all Cu surface atoms reside on sites between bridge and hollow sites, whereas the energetically expensive on top sites are avoided; i.e., the interface energy associated with the mismatch of surface layer and underlying bulk lattice is minimized. Several very similar $c(p \times 8)$ structures are possible, which only differ from each other by small lateral relaxations of the surface atoms and are difficult to distinguish on the basis of the current STM data.

Neither the simple stripe structure nor the Moiré superstructure has been reported in previous studies of atomic hydrogen adsorption on Cu(100) from the gas phase. Diffraction studies under UHV conditions reported different low-order commensurate superstructures with square symmetry at the hydrogen saturation coverage ($\sim$1 ML).[9−12] These measurements gave strong evidence for a surface reconstruction where the Cu surface atoms were laterally displaced from hollow sites, which was attributed to the presence of subsurface adsorbate species[10] or repulsive adsorbate interactions.[11] Furthermore, at the highest studied hydrogen exposure diffraction peaks at $^1/_4$ positions were found,[12] which were assigned to domain walls in the square superstructures, but also would be compatible with the stripe structure. However, an expanded Cu surface lattice involving a change in surface density was not reported up to now. Nevertheless, the structural similarity of the phases observed in the electrochemical environment as compared to those in UHV strongly suggests that they are likewise induced by adsorbed hydrogen on surface or subsurface sites. The remaining differences in the surface structures are most likely caused by the limited range of hydrogen partial pressure in the gas phase studies but may also be related to the lower temperatures required to adsorb hydrogen under UHV conditions or to the absence of water or other electrolyte species.

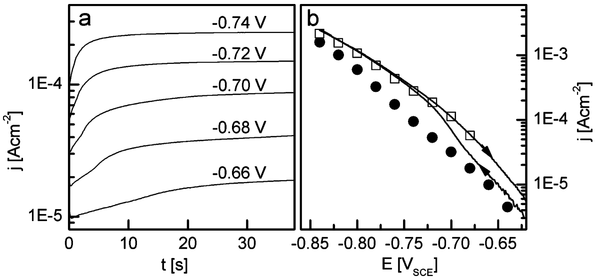

Figure 3. Electrochemical data for Cu(100) in 0.1 M $HClO_4$ solution. (a) Current transients during potential steps from -0.54 V_{SCE} to different potentials between -0.66 and -0.74 V_{SCE}. (b) Potential dependence of the current densities directly after the potential step (j_{in}, full circles) and after reaching saturation (j_{sat}, open squares) as well as a corresponding cyclic voltammogram at 2 mV/s potential sweep rate (solid line).

The surface reconstruction of the Cu(100) electrode strongly influences the kinetics of the hydrogen evolution reaction. Although cyclic voltammograms only exhibit a featureless increase in cathodic current, which can be associated with the HER,[13] the important influence of the reconstructed phase becomes evident in potential step experiments, showing that the HER current density initially has a low value j_{in} but subsequently strongly increases up to a saturation value j_{sat} (Figure 3a). The time to reach saturation decreases toward negative potentials, amounting to a few seconds only at potentials ≤ -0.74 V. This can be rationalized by an increasing formation rate of the surface reconstruction with decreasing potential, which is expected for phase transitions on electrode surfaces and in agreement with the STM observations. As visible in Figure 3b, j_{in} and j_{sat} exhibit a noticeably different potential dependence. Specifically, the data indicate that on the reconstructed surface the HER current density is increased but the Tafel slope (100 mV/decade) is decreased with respect to that on the (1×1) surface (83 mV/decade). The former indicates an enhanced electrocatalytic activity of the more open reconstructed Cu lattice, and the latter a change in the reaction mechanism. In Figure 3b also a corresponding cyclic voltammogram is included (solid line), which reveals a crossover from the behavior of a (1×1) to that of a reconstructed surface in the negative potential sweep, in accordance with the time dependence of the phase transition to the reconstructed surface. Furthermore, additional potential step experiments from the reconstructed phase into the double layer regime (see Supporting Information) reveal a small desorption peak with a charge of $\sim$6 $\mu C \cdot cm^{-2}$, much less than that expected for a hydrogen monolayer. This suggests that either hydrogen recombination to H_2 is favored over electrochemical desorption or that the surface reconstruction is stabilized by hydrogen coverages of a few percent only.

In summary, we have reported a novel hydrogen-induced reconstruction of the Cu(100) electrode surface structure and a concomitant increase in the hydrogen evolution reaction rate. Taking into account such structural changes under reaction conditions will be an important prerequisite for a true atomic scale understanding of electrochemical reactivity.

Acknowledgment. H.M. appreciates a scholarship from Japan Society for the Promotion Science. We gratefully acknowledge financial support by the Deutsche Forschungsgemeinschaft (MA 1618/14).

Supporting Information Available: Experimental procedures and additional electrochemical data. This material is available free of charge via the Internet at http://pubs.acs.org.

References

(1) Eberhardt, W.; Greuter, F.; Plummer, E. W. *Phys. Rev. Lett.* **1981**, *46*, 1085.
(2) Luo, M. F.; MacLaren, D. A.; Shuttleworth, I. G.; Allison, W. *Chem. Phys. Lett.* **2003**, *381*, 654.
(3) Jerkiewicz, G.; Zolfaghari, A. *J. Electrochem. Soc.* **1996**, *143*, 1240.
(4) Jerkiewicz, G. *Prog. Surf. Sci.* **1998**, *57*, 137.
(5) Besenbacher, F.; Stensgaard, I. In *The chemical physics of solid surfaces and heterogeneous catalysis*; King, D. A., Woodruff, D. P., Eds.; Elsevier Science Publishers: 1993.
(6) Kolb, D. M. *Prog. Surf. Sci.* **1996**, *51*, 109.
(7) Magnussen, O. M. *Chem. Rev.* **2002**, *102*, 679.
(8) Wilms, M.; Broekmann, P.; Stuhlmann, C.; Wandelt, K. *Surf. Sci.* **1998**, *416*, 121.
(9) Chorkendorff, I.; Rasmussen, P. B. *Surf. Sci.* **1991**, *248*, 35.
(10) Foss, M.; Besenbacher, F.; Klink, C.; Stensgaard, I. *Chem. Phys. Lett.* **1993**, *215*, 535.
(11) Graham, A. P.; McCash, E. M.; Allison, W. *Phys. Rev. B* **1995**, *51*, 5306.
(12) Graham, A. P.; Fang, D.; McCash, E. M.; Allison, W. *Phys. Rev. B* **1998**, *57*, 13158.
(13) Brisard, G.; Betrand, N.; Ross, P. N.; Markovic, N. M. *J. Electroanal. Chem.* **2000**, *480*, 219.

JA904033T